

Measurement of $B \rightarrow X\gamma$ Decays and Determination of $|V_{td}/V_{ts}|$

- B. Aubert,¹ M. Bona,¹ Y. Karyotakis,¹ J. P. Lees,¹ V. Poireau,¹ E. Prencipe,¹ X. Prudent,¹ V. Tisserand,¹ J. Garra Tico,² E. Grauges,² L. Lopez^{ab},³ A. Palano^{ab},³ M. Pappagallo^{ab},³ G. Eigen,⁴ B. Stugu,⁴ L. Sun,⁴ G. S. Abrams,⁵ M. Battaglia,⁵ D. N. Brown,⁵ R. N. Cahn,⁵ R. G. Jacobsen,⁵ L. T. Kerth,⁵ Yu. G. Kolomensky,⁵ G. Lynch,⁵ I. L. Osipenkov,⁵ M. T. Ronan,^{5,*} K. Tackmann,⁵ T. Tanabe,⁵ C. M. Hawkes,⁶ N. Soni,⁶ A. T. Watson,⁶ H. Koch,⁷ T. Schroeder,⁷ D. Walker,⁸ D. J. Asgeirsson,⁹ B. G. Fulson,⁹ C. Hearty,⁹ T. S. Mattison,⁹ J. A. McKenna,⁹ M. Barrett,¹⁰ A. Khan,¹⁰ V. E. Blinov,¹¹ A. D. Bokin,¹¹ A. R. Buzykaev,¹¹ V. P. Druzhinin,¹¹ V. B. Golubev,¹¹ A. P. Onuchin,¹¹ S. I. Serednyakov,¹¹ Yu. I. Skovpen,¹¹ E. P. Solodov,¹¹ K. Yu. Todyshev,¹¹ M. Bondioli,¹² S. Curry,¹² I. Eschrich,¹² D. Kirkby,¹² A. J. Lankford,¹² P. Lund,¹² M. Mandelkern,¹² E. C. Martin,¹² D. P. Stoker,¹² S. Abachi,¹³ C. Buchanan,¹³ J. W. Gary,¹⁴ F. Liu,¹⁴ O. Long,¹⁴ B. C. Shen,^{14,*} G. M. Vitug,¹⁴ Z. Yasin,¹⁴ L. Zhang,¹⁴ V. Sharma,¹⁵ C. Campagnari,¹⁶ T. M. Hong,¹⁶ D. Kovalskyi,¹⁶ M. A. Mazur,¹⁶ J. D. Richman,¹⁶ T. W. Beck,¹⁷ A. M. Eisner,¹⁷ C. J. Flacco,¹⁷ C. A. Heusch,¹⁷ J. Kroeseberg,¹⁷ W. S. Lockman,¹⁷ A. J. Martinez,¹⁷ T. Schalk,¹⁷ B. A. Schumm,¹⁷ A. Seiden,¹⁷ M. G. Wilson,¹⁷ L. O. Winstrom,¹⁷ C. H. Cheng,¹⁸ D. A. Doll,¹⁸ B. Echenard,¹⁸ F. Fang,¹⁸ D. G. Hitlin,¹⁸ I. Narsky,¹⁸ T. Piatenko,¹⁸ F. C. Porter,¹⁸ R. Andreassen,¹⁹ G. Mancinelli,¹⁹ B. T. Meadows,¹⁹ K. Mishra,¹⁹ M. D. Sokoloff,¹⁹ P. C. Bloom,²⁰ W. T. Ford,²⁰ A. Gaz,²⁰ J. F. Hirschauer,²⁰ M. Nagel,²⁰ U. Nauenberg,²⁰ J. G. Smith,²⁰ K. A. Ulmer,²⁰ S. R. Wagner,²⁰ R. Ayad,^{21,†} A. Soffer,^{21,‡} W. H. Toki,²¹ R. J. Wilson,²¹ D. D. Altenburg,²² E. Feltresi,²² A. Hauke,²² H. Jasper,²² M. Karbach,²² J. Merkel,²² A. Petzold,²² B. Spaan,²² K. Wacker,²² M. J. Kobel,²³ W. F. Mader,²³ R. Nogowski,²³ K. R. Schubert,²³ R. Schwierz,²³ A. Volk,²³ D. Bernard,²⁴ G. R. Bonneau,²⁴ E. Latour,²⁴ M. Verderi,²⁴ P. J. Clark,²⁵ S. Playfer,²⁵ J. E. Watson,²⁵ M. Andreotti^{ab},²⁶ D. Bettoni^a,²⁶ C. Bozzi^a,²⁶ R. Calabrese^{ab},²⁶ A. Cecchi^{ab},²⁶ G. Cibinetto^{ab},²⁶ P. Franchini^{ab},²⁶ E. Luppi^{ab},²⁶ M. Negrini^{ab},²⁶ A. Petrella^{ab},²⁶ L. Piemontese^a,²⁶ V. Santoro^{ab},²⁶ R. Baldini-Ferroli,²⁷ A. Calcaterra,²⁷ R. de Sangro,²⁷ G. Finocchiaro,²⁷ S. Pacetti,²⁷ P. Patteri,²⁷ I. M. Peruzzi,^{27,§} M. Piccolo,²⁷ M. Rama,²⁷ A. Zallo,²⁷ A. Buzzo^a,²⁸ R. Contri^{ab},²⁸ M. Lo Vetere^{ab},²⁸ M. M. Macri^a,²⁸ M. R. Monge^{ab},²⁸ S. Passaggio^a,²⁸ C. Patrignani^{ab},²⁸ E. Robutti^a,²⁸ A. Santroni^{ab},²⁸ S. Tosi^{ab},²⁸ K. S. Chaisanguanthum,²⁹ M. Morii,²⁹ A. Adametz,³⁰ J. Marks,³⁰ S. Schenck,³⁰ U. Uwer,³⁰ V. Klose,³¹ H. M. Lacker,³¹ D. J. Bard,³² P. D. Dauncey,³² J. A. Nash,³² M. Tibbetts,³² P. K. Behera,³³ X. Chai,³³ M. J. Charles,³³ U. Mallik,³³ J. Cochran,³⁴ H. B. Crawley,³⁴ L. Dong,³⁴ W. T. Meyer,³⁴ S. Prell,³⁴ E. I. Rosenberg,³⁴ A. E. Rubin,³⁴ Y. Y. Gao,³⁵ A. V. Gritsan,³⁵ Z. J. Guo,³⁵ C. K. Lae,³⁵ N. Arnaud,³⁶ J. Béquilleux,³⁶ A. D’Orazio,³⁶ M. Davier,³⁶ J. Firmino da Costa,³⁶ G. Grosdidier,³⁶ A. Höcker,³⁶ V. Lepeltier,³⁶ F. Le Diberder,³⁶ A. M. Lutz,³⁶ S. Pruvot,³⁶ P. Roudeau,³⁶ M. H. Schune,³⁶ J. Serrano,³⁶ V. Sordini,^{36,¶} A. Stocchi,³⁶ G. Wormser,³⁶ D. J. Lange,³⁷ D. M. Wright,³⁷ I. Bingham,³⁸ J. P. Burke,³⁸ C. A. Chavez,³⁸ J. R. Fry,³⁸ E. Gabathuler,³⁸ R. Gamet,³⁸ D. E. Hutchcroft,³⁸ D. J. Payne,³⁸ C. Touramanis,³⁸ A. J. Bevan,³⁹ C. K. Clarke,³⁹ K. A. George,³⁹ F. Di Lodovico,³⁹ R. Sacco,³⁹ M. Sigamani,³⁹ G. Cowan,⁴⁰ H. U. Flaecher,⁴⁰ D. A. Hopkins,⁴⁰ S. Paramesvaran,⁴⁰ F. Salvatore,⁴⁰ A. C. Wren,⁴⁰ D. N. Brown,⁴¹ C. L. Davis,⁴¹ A. G. Denig,⁴² M. Fritsch,⁴² W. Gradl,⁴² G. Schott,⁴² K. E. Alwyn,⁴³ D. Bailey,⁴³ R. J. Barlow,⁴³ Y. M. Chia,⁴³ C. L. Edgar,⁴³ G. Jackson,⁴³ G. D. Lafferty,⁴³ T. J. West,⁴³ J. I. Yi,⁴³ J. Anderson,⁴⁴ C. Chen,⁴⁴ A. Jawahery,⁴⁴ D. A. Roberts,⁴⁴ G. Simi,⁴⁴ J. M. Tuggle,⁴⁴ C. Dallapiccola,⁴⁵ X. Li,⁴⁵ E. Salvati,⁴⁵ S. Saremi,⁴⁵ R. Cowan,⁴⁶ D. Dujmic,⁴⁶ P. H. Fisher,⁴⁶ G. Sciolla,⁴⁶ M. Spitznagel,⁴⁶ F. Taylor,⁴⁶ R. K. Yamamoto,⁴⁶ M. Zhao,⁴⁶ P. M. Patel,⁴⁷ S. H. Robertson,⁴⁷ A. Lazzaro^{ab},⁴⁸ V. Lombardo^a,⁴⁸ F. Palombo^{ab},⁴⁸ J. M. Bauer,⁴⁹ L. Cremaldi,⁴⁹ R. Godang,^{49,**} R. Kroeger,⁴⁹ D. A. Sanders,⁴⁹ D. J. Summers,⁴⁹ H. W. Zhao,⁴⁹ M. Simard,⁵⁰ P. Taras,⁵⁰ F. B. Viaud,⁵⁰ H. Nicholson,⁵¹ G. De Nardo^{ab},⁵² L. Lista^a,⁵² D. Monorchio^{ab},⁵² G. Onorato^{ab},⁵² C. Sciacca^{ab},⁵² G. Raven,⁵³ H. L. Snoek,⁵³ C. P. Jessop,⁵⁴ K. J. Knoepfel,⁵⁴ J. M. LoSecco,⁵⁴ W. F. Wang,⁵⁴ G. Benelli,⁵⁵ L. A. Corwin,⁵⁵ K. Honscheid,⁵⁵ H. Kagan,⁵⁵ R. Kass,⁵⁵ J. P. Morris,⁵⁵ A. M. Rahimi,⁵⁵ J. J. Regensburger,⁵⁵ S. J. Sekula,⁵⁵ Q. K. Wong,⁵⁵ N. L. Blount,⁵⁶ J. Brau,⁵⁶ R. Frey,⁵⁶ O. Igonkina,⁵⁶ J. A. Kolb,⁵⁶ M. Lu,⁵⁶ R. Rahmat,⁵⁶ N. B. Sinev,⁵⁶ D. Strom,⁵⁶ J. Strube,⁵⁶ E. Torrence,⁵⁶ G. Castelli^{ab},⁵⁷ N. Gagliardi^{ab},⁵⁷ M. Margoni^{ab},⁵⁷ M. Morandin^a,⁵⁷ M. Posocco^a,⁵⁷ M. Rotondo^a,⁵⁷ F. Simonetto^{ab},⁵⁷ R. Stroili^{ab},⁵⁷ C. Voci^{ab},⁵⁷ P. del Amo Sanchez,⁵⁸ E. Ben-Haim,⁵⁸ H. Briand,⁵⁸ G. Calderini,⁵⁸ J. Chauveau,⁵⁸ P. David,⁵⁸ L. Del Buono,⁵⁸ O. Hamon,⁵⁸ Ph. Leruste,⁵⁸ J. Ocariz,⁵⁸ A. Perez,⁵⁸ J. Prendki,⁵⁸ S. Sitt,⁵⁸ L. Gladney,⁵⁹ M. Biasini^{ab},⁶⁰ R. Covarelli^{ab},⁶⁰ E. Manoni^{ab},⁶⁰ C. Angelini^{ab},⁶¹ G. Batignani^{ab},⁶¹ S. Bettarini^{ab},⁶¹ M. Carpinelli^{ab},^{61,††}

- A. Cervelli^{ab},⁶¹ F. Forti^{ab},⁶¹ M. A. Giorgi^{ab},⁶¹ A. Lusiani^{ac},⁶¹ G. Marchiori^{ab},⁶¹ M. Morganti^{ab},⁶¹ N. Neri^{ab},⁶¹
 E. Paoloni^{ab},⁶¹ G. Rizzo^{ab},⁶¹ J. J. Walsh^a,⁶¹ D. Lopes Pegna,⁶² C. Lu,⁶² J. Olsen,⁶² A. J. S. Smith,⁶²
 A. V. Telnov,⁶² F. Anulli^a,⁶³ E. Baracchini^{ab},⁶³ G. Cavoto^a,⁶³ D. del Re^{ab},⁶³ E. Di Marco^{ab},⁶³ R. Faccini^{ab},⁶³
 F. Ferrarotto^a,⁶³ F. Ferroni^{ab},⁶³ M. Gaspero^{ab},⁶³ P. D. Jackson^a,⁶³ L. Li Gioi^a,⁶³ M. A. Mazzoni^a,⁶³ S. Morganti^a,⁶³
 G. Piredda^a,⁶³ F. Polci^{ab},⁶³ F. Renga^{ab},⁶³ C. Voena^a,⁶³ M. Ebert,⁶⁴ T. Hartmann,⁶⁴ H. Schröder,⁶⁴ R. Waldi,⁶⁴
 T. Adye,⁶⁵ B. Franek,⁶⁵ E. O. Olaiya,⁶⁵ F. F. Wilson,⁶⁵ S. Emery,⁶⁶ M. Escalier,⁶⁶ L. Esteve,⁶⁶ S. F. Ganzhur,⁶⁶
 G. Hamel de Monchenault,⁶⁶ W. Kozanecki,⁶⁶ G. Vasseur,⁶⁶ Ch. Yèche,⁶⁶ M. Zito,⁶⁶ X. R. Chen,⁶⁷ H. Liu,⁶⁷
 W. Park,⁶⁷ M. V. Purohit,⁶⁷ R. M. White,⁶⁷ J. R. Wilson,⁶⁷ M. T. Allen,⁶⁸ D. Aston,⁶⁸ R. Bartoldus,⁶⁸
 P. Bechtle,⁶⁸ J. F. Benitez,⁶⁸ R. Cenci,⁶⁸ J. P. Coleman,⁶⁸ M. R. Convery,⁶⁸ J. C. Dingfelder,⁶⁸ J. Dorfan,⁶⁸
 G. P. Dubois-Felsmann,⁶⁸ W. Dunwoodie,⁶⁸ R. C. Field,⁶⁸ A. M. Gabareen,⁶⁸ S. J. Gowdy,⁶⁸ M. T. Graham,⁶⁸
 P. Grenier,⁶⁸ C. Hast,⁶⁸ W. R. Innes,⁶⁸ J. Kaminski,⁶⁸ M. H. Kelsey,⁶⁸ H. Kim,⁶⁸ P. Kim,⁶⁸ M. L. Kocian,⁶⁸
 D. W. G. S. Leith,⁶⁸ S. Li,⁶⁸ B. Lindquist,⁶⁸ S. Luitz,⁶⁸ V. Luth,⁶⁸ H. L. Lynch,⁶⁸ D. B. MacFarlane,⁶⁸
 H. Marsiske,⁶⁸ R. Messner,⁶⁸ D. R. Muller,⁶⁸ H. Neal,⁶⁸ S. Nelson,⁶⁸ C. P. O'Grady,⁶⁸ I. Ofte,⁶⁸ A. Perazzo,⁶⁸
 M. Perl,⁶⁸ B. N. Ratcliff,⁶⁸ A. Roodman,⁶⁸ A. A. Salnikov,⁶⁸ R. H. Schindler,⁶⁸ J. Schwiening,⁶⁸ A. Snyder,⁶⁸
 D. Su,⁶⁸ M. K. Sullivan,⁶⁸ K. Suzuki,⁶⁸ S. K. Swain,⁶⁸ J. M. Thompson,⁶⁸ J. Va'vra,⁶⁸ A. P. Wagner,⁶⁸
 M. Weaver,⁶⁸ C. A. West,⁶⁸ W. J. Wisniewski,⁶⁸ M. Wittgen,⁶⁸ D. H. Wright,⁶⁸ H. W. Wulsen,⁶⁸ A. K. Yarritu,⁶⁸
 K. Yi,⁶⁸ C. C. Young,⁶⁸ V. Ziegler,⁶⁸ P. R. Burchat,⁶⁹ A. J. Edwards,⁶⁹ S. A. Majewski,⁶⁹ T. S. Miyashita,⁶⁹
 B. A. Petersen,⁶⁹ L. Wilden,⁶⁹ S. Ahmed,⁷⁰ M. S. Alam,⁷⁰ J. A. Ernst,⁷⁰ B. Pan,⁷⁰ M. A. Saeed,⁷⁰ S. B. Zain,⁷⁰
 S. M. Spanier,⁷¹ B. J. Wogsland,⁷¹ R. Eckmann,⁷² J. L. Ritchie,⁷² A. M. Ruland,⁷² C. J. Schilling,⁷²
 R. F. Schwitters,⁷² B. W. Drummond,⁷³ J. M. Izen,⁷³ X. C. Lou,⁷³ F. Bianchi^{ab},⁷⁴ D. Gamba^{ab},⁷⁴ M. Pelliccioni^{ab},⁷⁴
 M. Bomben^{ab},⁷⁵ L. Bosisio^{ab},⁷⁵ C. Cartaro^{ab},⁷⁵ G. Della Ricca^{ab},⁷⁵ L. Lanceri^{ab},⁷⁵ L. Vitale^{ab},⁷⁵ V. Azzolini,⁷⁶
 N. Lopez-March,⁷⁶ F. Martinez-Vidal,⁷⁶ D. A. Milanes,⁷⁶ A. Oyanguren,⁷⁶ J. Albert,⁷⁷ Sw. Banerjee,⁷⁷
 B. Bhuyan,⁷⁷ H. H. F. Choi,⁷⁷ K. Hamano,⁷⁷ R. Kowalewski,⁷⁷ M. J. Lewczuk,⁷⁷ I. M. Nugent,⁷⁷ J. M. Roney,⁷⁷
 R. J. Sobie,⁷⁷ T. J. Gershon,⁷⁸ P. F. Harrison,⁷⁸ J. Ilic,⁷⁸ T. E. Latham,⁷⁸ G. B. Mohanty,⁷⁸ H. R. Band,⁷⁹
 X. Chen,⁷⁹ S. Dasu,⁷⁹ K. T. Flood,⁷⁹ Y. Pan,⁷⁹ M. Pierini,⁷⁹ R. Prepost,⁷⁹ C. O. Vuosalo,⁷⁹ and S. L. Wu⁷⁹

(The BABAR Collaboration)

¹Laboratoire de Physique des Particules, IN2P3/CNRS et Université de Savoie, F-74941 Annecy-Le-Vieux, France

²Universitat de Barcelona, Facultat de Fisica, Departament ECM, E-08028 Barcelona, Spain

³INFN Sezione di Bari^a; Dipartimento di Fisica, Università di Bari^b, I-70126 Bari, Italy

⁴University of Bergen, Institute of Physics, N-5007 Bergen, Norway

⁵Lawrence Berkeley National Laboratory and University of California, Berkeley, California 94720, USA

⁶University of Birmingham, Birmingham, B15 2TT, United Kingdom

⁷Ruhr Universität Bochum, Institut für Experimentalphysik 1, D-44780 Bochum, Germany

⁸University of Bristol, Bristol BS8 1TL, United Kingdom

⁹University of British Columbia, Vancouver, British Columbia, Canada V6T 1Z1

¹⁰Brunel University, Uxbridge, Middlesex UB8 3PH, United Kingdom

¹¹Budker Institute of Nuclear Physics, Novosibirsk 630090, Russia

¹²University of California at Irvine, Irvine, California 92697, USA

¹³University of California at Los Angeles, Los Angeles, California 90024, USA

¹⁴University of California at Riverside, Riverside, California 92521, USA

¹⁵University of California at San Diego, La Jolla, California 92093, USA

¹⁶University of California at Santa Barbara, Santa Barbara, California 93106, USA

¹⁷University of California at Santa Cruz, Institute for Particle Physics, Santa Cruz, California 95064, USA

¹⁸California Institute of Technology, Pasadena, California 91125, USA

¹⁹University of Cincinnati, Cincinnati, Ohio 45221, USA

²⁰University of Colorado, Boulder, Colorado 80309, USA

²¹Colorado State University, Fort Collins, Colorado 80523, USA

²²Technische Universität Dortmund, Fakultät Physik, D-44221 Dortmund, Germany

²³Technische Universität Dresden, Institut für Kern- und Teilchenphysik, D-01062 Dresden, Germany

²⁴Laboratoire Leprince-Ringuet, CNRS/IN2P3, Ecole Polytechnique, F-91128 Palaiseau, France

²⁵University of Edinburgh, Edinburgh EH9 3JZ, United Kingdom

²⁶INFN Sezione di Ferrara^a; Dipartimento di Fisica, Università di Ferrara^b, I-44100 Ferrara, Italy

²⁷INFN Laboratori Nazionali di Frascati, I-00044 Frascati, Italy

²⁸INFN Sezione di Genova^a; Dipartimento di Fisica, Università di Genova^b, I-16146 Genova, Italy

²⁹Harvard University, Cambridge, Massachusetts 02138, USA

³⁰Universität Heidelberg, Physikalisches Institut, Philosophenweg 12, D-69120 Heidelberg, Germany

³¹Humboldt-Universität zu Berlin, Institut für Physik, Newtonstr. 15, D-12489 Berlin, Germany

³²Imperial College London, London, SW7 2AZ, United Kingdom

- ³³University of Iowa, Iowa City, Iowa 52242, USA
³⁴Iowa State University, Ames, Iowa 50011-3160, USA
³⁵Johns Hopkins University, Baltimore, Maryland 21218, USA
³⁶Laboratoire de l'Accélérateur Linéaire, IN2P3/CNRS et Université Paris-Sud 11, Centre Scientifique d'Orsay, B. P. 34, F-91898 Orsay Cedex, France
³⁷Lawrence Livermore National Laboratory, Livermore, California 94550, USA
³⁸University of Liverpool, Liverpool L69 7ZE, United Kingdom
³⁹Queen Mary, University of London, London, E1 4NS, United Kingdom
⁴⁰University of London, Royal Holloway and Bedford New College, Egham, Surrey TW20 0EX, United Kingdom
⁴¹University of Louisville, Louisville, Kentucky 40292, USA
⁴²Johannes Gutenberg-Universität Mainz, Institut für Kernphysik, D-55099 Mainz, Germany
⁴³University of Manchester, Manchester M13 9PL, United Kingdom
⁴⁴University of Maryland, College Park, Maryland 20742, USA
⁴⁵University of Massachusetts, Amherst, Massachusetts 01003, USA
⁴⁶Massachusetts Institute of Technology, Laboratory for Nuclear Science, Cambridge, Massachusetts 02139, USA
⁴⁷McGill University, Montréal, Québec, Canada H3A 2T8
⁴⁸INFN Sezione di Milano^a; Dipartimento di Fisica, Università di Milano^b, I-20133 Milano, Italy
⁴⁹University of Mississippi, University, Mississippi 38677, USA
⁵⁰Université de Montréal, Physique des Particules, Montréal, Québec, Canada H3C 3J7
⁵¹Mount Holyoke College, South Hadley, Massachusetts 01075, USA
⁵²INFN Sezione di Napoli^a; Dipartimento di Scienze Fisiche, Università di Napoli Federico II^b, I-80126 Napoli, Italy
⁵³NIKHEF, National Institute for Nuclear Physics and High Energy Physics, NL-1009 DB Amsterdam, The Netherlands
⁵⁴University of Notre Dame, Notre Dame, Indiana 46556, USA
⁵⁵Ohio State University, Columbus, Ohio 43210, USA
⁵⁶University of Oregon, Eugene, Oregon 97403, USA
⁵⁷INFN Sezione di Padova^a; Dipartimento di Fisica, Università di Padova^b, I-35131 Padova, Italy
⁵⁸Laboratoire de Physique Nucléaire et de Hautes Energies, IN2P3/CNRS, Université Pierre et Marie Curie-Paris6, Université Denis Diderot-Paris7, F-75252 Paris, France
⁵⁹University of Pennsylvania, Philadelphia, Pennsylvania 19104, USA
⁶⁰INFN Sezione di Perugia^a; Dipartimento di Fisica, Università di Perugia^b, I-06100 Perugia, Italy
⁶¹INFN Sezione di Pisa^a; Dipartimento di Fisica, Università di Pisa^b; Scuola Normale Superiore di Pisa^c, I-56127 Pisa, Italy
⁶²Princeton University, Princeton, New Jersey 08544, USA
⁶³INFN Sezione di Roma^a; Dipartimento di Fisica, Università di Roma La Sapienza^b, I-00185 Roma, Italy
⁶⁴Universität Rostock, D-18051 Rostock, Germany
⁶⁵Rutherford Appleton Laboratory, Chilton, Didcot, Oxon, OX11 0QX, United Kingdom
⁶⁶CEA, Ifu, SPP, Centre de Saclay, F-91191 Gif-sur-Yvette, France
⁶⁷University of South Carolina, Columbia, South Carolina 29208, USA
⁶⁸Stanford Linear Accelerator Center, Stanford, California 94309, USA
⁶⁹Stanford University, Stanford, California 94305-4060, USA
⁷⁰State University of New York, Albany, New York 12222, USA
⁷¹University of Tennessee, Knoxville, Tennessee 37996, USA
⁷²University of Texas at Austin, Austin, Texas 78712, USA
⁷³University of Texas at Dallas, Richardson, Texas 75083, USA
⁷⁴INFN Sezione di Torino^a; Dipartimento di Fisica Sperimentale, Università di Torino^b, I-10125 Torino, Italy
⁷⁵INFN Sezione di Trieste^a; Dipartimento di Fisica, Università di Trieste^b, I-34127 Trieste, Italy
⁷⁶IFIC, Universitat de Valencia-CSIC, E-46071 Valencia, Spain
⁷⁷University of Victoria, Victoria, British Columbia, Canada V8W 3P6
⁷⁸Department of Physics, University of Warwick, Coventry CV4 7AL, United Kingdom
⁷⁹University of Wisconsin, Madison, Wisconsin 53706, USA

(Dated: August 1, 2008)

Using a sample of 383 million $B\bar{B}$ events collected by the *BABAR* experiment, we measure sums of seven exclusive final states $B \rightarrow X_{d(s)}\gamma$, where $X_d(X_s)$ is a non-strange (strange) charmless hadronic system in the mass range $0.6 - 1.8 \text{ GeV}/c^2$. After correcting for unmeasured decay modes in this mass range, we obtain a branching fraction for $b \rightarrow d\gamma$ of $(7.2 \pm 2.7(\text{stat.}) \pm 2.3(\text{syst.})) \times 10^{-6}$. Taking the ratio of X_d to X_s we find $\Gamma(b \rightarrow d\gamma)/\Gamma(b \rightarrow s\gamma) = 0.033 \pm 0.013(\text{stat.}) \pm 0.009(\text{syst.})$, from which we determine $|V_{td}/V_{ts}| = 0.177 \pm 0.043$.

The decays $b \rightarrow d\gamma$ and $b \rightarrow s\gamma$ are flavor-changing neutral current processes forbidden at tree level in the standard model (SM). The leading-order processes are one-loop electroweak penguin diagrams in which the top quark is the dominant virtual particle. In the SM the inclusive rate for $b \rightarrow d\gamma$ is suppressed compared to $b \rightarrow s\gamma$ by a factor of $|V_{td}/V_{ts}|^2$, where V_{td} and V_{ts} are Cabibbo-Kobayashi-Maskawa matrix elements. Measurements of $|V_{td}/V_{ts}|$ using the exclusive modes $B \rightarrow (\rho, \omega)\gamma$ and $B \rightarrow K^*\gamma$ [1] have theoretical uncertainties of 7% from weak annihilation and hadronic form factors [2]. A measurement of the inclusive decay $b \rightarrow d\gamma$ relative to $b \rightarrow s\gamma$ could determine $|V_{td}/V_{ts}|$ with reduced theoretical uncertainties compared to the exclusive modes [3]. In theories beyond the SM [4], new virtual particles may appear differently in the penguin loop diagrams for $b \rightarrow d\gamma$ and $b \rightarrow s\gamma$ and in the box diagrams responsible for B_d and B_s mixing [5], leading to measurable differences in $|V_{td}/V_{ts}|$ extracted from these two methods.

We present measurements of the rare decays $B \rightarrow X_d\gamma$ using seven exclusive final states (see Table I) in the hadronic mass range $0.6 < M(X_d) < 1.0 \text{ GeV}/c^2$ (which contains the ρ and ω resonances), and in the previously unmeasured region $1.0 < M(X_d) < 1.8 \text{ GeV}/c^2$. We combine our results in the two mass regions and make corrections for decay modes that are not reconstructed to obtain an inclusive branching fraction for $b \rightarrow d\gamma$ in the mass range 0.6 - $1.8 \text{ GeV}/c^2$. We perform a parallel analysis of $B \rightarrow X_s\gamma$ using the equivalent seven modes (Table I), and determine the ratio of inclusive rates $\Gamma(b \rightarrow d\gamma)/\Gamma(b \rightarrow s\gamma)$ in the hadronic mass range $0.6 < M(X_d) < 1.8 \text{ GeV}/c^2$.

These measurements use a sample of 383×10^6 $B\bar{B}$

TABLE I: The reconstructed decay modes. Charge conjugate states are implied throughout this paper.

$B \rightarrow X_d\gamma$	$B \rightarrow X_s\gamma$
$B^0 \rightarrow \pi^+ \pi^- \gamma$	$B^0 \rightarrow K^+ \pi^- \gamma$
$B^+ \rightarrow \pi^+ \pi^0 \gamma$	$B^+ \rightarrow K^+ \pi^0 \gamma$
$B^+ \rightarrow \pi^+ \pi^- \pi^+ \gamma$	$B^+ \rightarrow K^+ \pi^- \pi^+ \gamma$
$B^0 \rightarrow \pi^+ \pi^- \pi^0 \gamma$	$B^0 \rightarrow K^+ \pi^- \pi^0 \gamma$
$B^0 \rightarrow \pi^+ \pi^- \pi^+ \pi^- \gamma$	$B^0 \rightarrow K^+ \pi^- \pi^+ \pi^- \gamma$
$B^+ \rightarrow \pi^+ \pi^- \pi^+ \pi^0 \gamma$	$B^+ \rightarrow K^+ \pi^- \pi^+ \pi^0 \gamma$
$B^+ \rightarrow \pi^+ \eta \gamma$	$B^+ \rightarrow K^+ \eta \gamma$

*Deceased

†Now at Temple University, Philadelphia, Pennsylvania 19122, USA

‡Now at Tel Aviv University, Tel Aviv, 69978, Israel

§Also with Università di Perugia, Dipartimento di Fisica, Perugia, Italy

¶Also with Università di Roma La Sapienza, I-00185 Roma, Italy

**Now at University of South Alabama, Mobile, Alabama 36688, USA

††Also with Università di Sassari, Sassari, Italy

pairs collected at the $\Upsilon(4S)$ resonance with the *BABAR* detector [6] at the PEP-II B factory. The high-energy photon is reconstructed from an isolated energy cluster in the CsI(Tl) calorimeter, which has a shape consistent with a single photon, and an energy $1.15 < E_\gamma^* < 3.5 \text{ GeV}$ in the center-of-mass (CM) frame. We remove photons that can form a π^0 (η) candidate with another photon of energy greater than 30 (250) MeV, if the two-photon invariant mass is in the range $105 < m_{\gamma\gamma} < 155 \text{ MeV}/c^2$ ($500 < m_{\gamma\gamma} < 590 \text{ MeV}/c^2$).

Charged pion and kaon candidates are measured in a 1.5 T magnetic field as tracks in a 5-layer silicon vertex detector and a 40-layer drift chamber, with a minimum momentum in the laboratory frame of $300 \text{ MeV}/c$. To differentiate pions from kaons we combine information from the detector of internally reflected Cherenkov light with the energy loss measured in the tracking system. At a typical pion energy of 1 GeV, the pion selection efficiency is 85% and the kaon mis-identification rate is 3%. Kaons are selected by inverting the pion selection criteria. We reconstruct $\pi^0(\eta)$ candidates with momenta greater than $300 \text{ MeV}/c$ from pairs of photons of minimum energy 20 MeV with an invariant mass $107 < m_{\gamma\gamma} < 145 \text{ MeV}/c^2$ ($470 < m_{\gamma\gamma} < 620 \text{ MeV}/c^2$). The selected charged tracks, $\pi^0(\eta)$ candidates, and high-energy photons are combined to form B meson candidates consistent with one of the seven $B \rightarrow X_s\gamma$ or $B \rightarrow X_d\gamma$ decay modes. For $B \rightarrow X_s\gamma$ decays one charged kaon is required, with all other tracks required to be pions. For $B \rightarrow X_d\gamma$ decays, all tracks are required to be identified as pions. The charged particles are combined to form a common vertex with a vertex fit probability greater than 2%.

Most of the backgrounds in this analysis arise from continuum $e^+e^- \rightarrow q\bar{q}$ events, $q = (u, d, s, c)$, in which a high-energy photon comes from either initial state radiation or the decay of a $\pi^0(\eta)$ meson. We require $R_2 < 0.9$ and $|\cos \theta_T| < 0.8$, where R_2 is the ratio of the second to zeroth Fox-Wolfram moments [7], and θ_T is the angle between the photon and the thrust axis of the rest of the event (ROE) in the CM frame. The ROE includes all the charged tracks and neutral energy in the calorimeter not used to reconstruct the B candidate.

The quantity $\cos \theta_T$ and twelve other variables that distinguish between signal and continuum events are combined in a neural network (NN). These include the ratio R'_2 , which is R_2 is calculated in the frame recoiling against the photon momentum, the B meson production angle θ_B^* in the CM frame with respect to the beam axis, and five Legendre moments of the ROE with respect to both the thrust axis of the ROE, and the direction of the high-energy photon. Differences in lepton and kaon production between background and B decays are exploited by including five flavor-tagging variables applied to the ROE [8]. We optimize the NN configuration for maximal discrimination between signal and continuum background, which gives 50% signal efficiency and 0.5% misidentification of continuum background.

We use the kinematic variables $\Delta E = E_B^* - E_{\text{beam}}^*$ and

$m_{ES} = \sqrt{E_{beam}^{*2} - |\vec{p}_B^{*2}|}$, where E_B^* and \vec{p}_B^* are the CM energy and momentum of the B candidate, and E_{beam}^* is the CM energy of one beam. Signal events are expected to have a ΔE distribution centered at zero with a resolution of about 30 MeV, and an m_{ES} distribution centered at the mass of the B meson with a resolution of about 3 MeV/c 2 . We consider candidates in the ranges $-0.3 \text{ GeV} < \Delta E < 0.2 \text{ GeV}$ and $m_{ES} > 5.22 \text{ GeV}/c^2$ to incorporate sidebands that allow the combinatorial background yields to be extracted from a fit to the data. On average there are 1.75 candidates per event, and in events with multiple candidates we select the one with the best $\pi^0(\eta)$ mass, or, where there is no $\pi^0(\eta)$ we select the candidate with the best vertex fit probability.

The signal yields in the data are determined from two-dimensional unbinned maximum likelihood fits to the ΔE and m_{ES} distributions of the sums of all seven final states listed in Table I. We consider the following contributions: signal, combinatorial backgrounds from continuum processes, $B \rightarrow X\pi^0/\eta$ decays, backgrounds from other B decays, and cross-feed from mis-reconstructed signal $B \rightarrow X\gamma$ decays. The fits to the $B \rightarrow X_d\gamma$ samples contain a component from misidentified $B \rightarrow X_s\gamma$ decays, but we neglect the small $B \rightarrow X_d\gamma$ background in the $B \rightarrow X_s\gamma$ samples. The B background yields are determined from a Monte Carlo (MC) simulation, whereas the continuum background is allowed to float in the fit.

Each background contribution is modeled by a probability density function (PDF) that is determined from MC. The signal PDFs are the product of one-dimensional m_{ES} and ΔE distributions determined from fits to the $B \rightarrow K^*\gamma$ data. For the signal cross-feed component, and the $B \rightarrow X_s\gamma$ background in the $B \rightarrow X_d\gamma$ fit, we use two-dimensional histogram PDFs to account for correlations. The contributions from $B \rightarrow X\pi^0/\eta$ are modeled by Gaussian peaks in both ΔE and m_{ES} , where ΔE is displaced by -80 MeV due to the missing photon. The $B \rightarrow X_s\gamma$ background in the $B \rightarrow X_d\gamma$ sample also peaks with ΔE displaced by -50 MeV due to the kaon misidentification. Continuum and other non-peaking backgrounds are described by an ARGUS shape [9] in m_{ES} and a second-order polynomial in ΔE .

We perform fits separately for $B \rightarrow X_d\gamma$ and $B \rightarrow X_s\gamma$ and in the two hadronic mass ranges. The signal and continuum yields and the ARGUS and polynomial continuum shape parameters are allowed to vary. We scale the cross-feed contribution proportionally to the fitted signal yield, re-fit, and iterate until the fit converges. The fits for $B \rightarrow X_s\gamma$ and $B \rightarrow X_d\gamma$ are shown in the low- and high-mass regions in Figs. 1 and 2, respectively.

The signal yields, average efficiencies and partial branching fractions for the sums of the seven decay modes are given in Table II. The reconstruction efficiency depends on the distribution of the signal yield among the final states. For X_s we measure the distribution of the final states in the data, but for X_d there is no statistically useful information, so we model the distribution using the phase space fragmentation model implemented

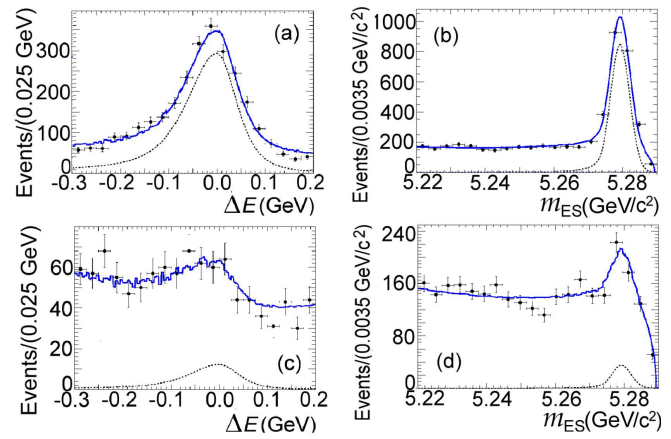


FIG. 1: Projections of the fits to data in the hadronic mass range $0.6\text{--}1.0 \text{ GeV}/c^2$. Projection of ΔE with $5.275 < m_{ES} < 5.286 \text{ GeV}/c^2$ for (a) $B \rightarrow X_s\gamma$ and (c) $B \rightarrow X_d\gamma$, and m_{ES} with $-0.1 < \Delta E < 0.05 \text{ GeV}$ for (b) $B \rightarrow X_s\gamma$ and (d) $B \rightarrow X_d\gamma$. Data points are compared with the sum of all the fit contributions (solid line) including the signal (dashed line).

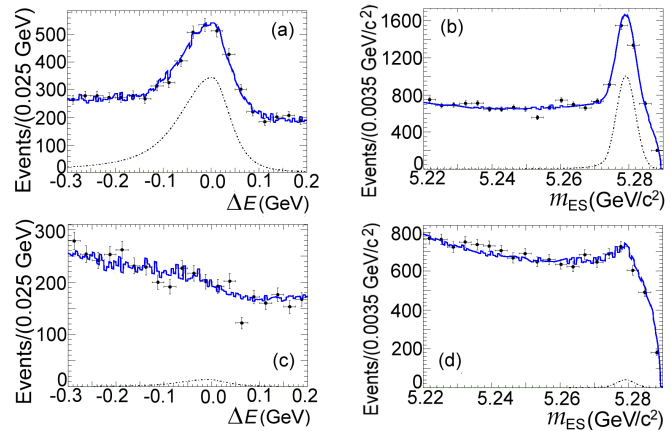


FIG. 2: Projections of the fits to data in the hadronic mass range $1.0\text{--}1.8 \text{ GeV}/c^2$. Projection of ΔE with $5.275 < m_{ES} < 5.286 \text{ GeV}/c^2$ for (a) $B \rightarrow X_s\gamma$ and (c) $B \rightarrow X_d\gamma$, and m_{ES} with $-0.1 < \Delta E < 0.05 \text{ GeV}$ for (b) $B \rightarrow X_s\gamma$ and (d) $B \rightarrow X_d\gamma$. Data points are compared with the sum of all the fit contributions (solid line) including the signal (dashed line).

in JETSET [10].

The branching fractions in Table III are obtained after correcting for missing final states. The low mass $B \rightarrow X_s\gamma$ measurement is found to be consistent with previous measurements of the rate for $B \rightarrow K^*\gamma$ [11], after accounting for the 50% of decays to neutral kaons. For the low mass $B \rightarrow X_d\gamma$ region, non-reconstructed ρ and ω decays are small and we find a branching fraction of $(1.2 \pm 0.5) \times 10^{-6}$, consistent with previous measurements of $\mathcal{B}(B \rightarrow (\rho, \omega)\gamma)$ [1]. In the high mass region, we correct for missing final states with ≥ 5 stable particles, or with multiple π^0 's, using the fragmentation model

TABLE II: Signal yields (N_S), average efficiencies (ϵ) and partial branching fractions (\mathcal{B}) for the measured decay modes. The first error is statistical, the second systematic.

$M(X)[\text{GeV}/c^2]$	N_S	ϵ	$\mathcal{B}(\times 10^{-6})$
$0.6 < M(X_s) < 1.0$	1543 ± 46	8.5%	$23.7 \pm 0.7 \pm 1.7$
$0.6 < M(X_d) < 1.0$	66 ± 26	7.0%	$1.2 \pm 0.5 \pm 0.1$
$1.0 < M(X_s) < 1.8$	2279 ± 75	6.1%	$48.7 \pm 1.6 \pm 4.1$
$1.0 < M(X_d) < 1.8$	107 ± 47	5.2%	$2.7 \pm 1.2 \pm 0.4$

TABLE III: Branching fractions $\mathcal{B}(\times 10^{-6})$ in the two hadronic mass regions $M(X)[\text{GeV}/c^2]$, after correcting for missing final states, and the ratios of $\mathcal{B}(b \rightarrow d\gamma)$ to $\mathcal{B}(b \rightarrow s\gamma)$. The first errors are statistical, and the second are systematic, including the fragmentation of the hadronic system.

$M(X)$	$\mathcal{B}(b \rightarrow d\gamma)$	$\mathcal{B}(b \rightarrow s\gamma)$	$\mathcal{B}(b \rightarrow d\gamma)/\mathcal{B}(b \rightarrow s\gamma)$
$0.6 - 1.0$	$1.2 \pm 0.5 \pm 0.1$	$47 \pm 1 \pm 3$	$0.026 \pm 0.011 \pm 0.002$
$1.0 - 1.8$	$6.0 \pm 2.6 \pm 2.3$	$168 \pm 14 \pm 33$	$0.036 \pm 0.015 \pm 0.009$
$0.6 - 1.8$	$7.2 \pm 2.7 \pm 2.3$	$215 \pm 14 \pm 33$	$0.033 \pm 0.013 \pm 0.009$

described above.

The sources of systematic uncertainties in the measurement of the branching fractions are listed in Table IV. These include uncertainties on track reconstruction efficiency, γ and π^0/η reconstruction, the π^0/η veto, the NN selection, and the number of $B\bar{B}$ pairs. The 2% uncertainty on correct kaon/pion particle identification, and the 20% uncertainty on kaon misidentification, which is a systematic on the fixed $b \rightarrow s\gamma$ background in the $B \rightarrow X_d\gamma$ fits, do not cancel in the ratio. The systematic errors associated with the variation of the fit PDFs also do not cancel because of the very different signal

TABLE IV: Systematic errors on the measured partial and total branching fractions \mathcal{B} . The final column shows systematic errors that do not cancel in the ratio of rates $\Gamma(b \rightarrow d\gamma)/\Gamma(b \rightarrow s\gamma)$.

Systematic Error Source	$M(X_s)$		$M(X_d)$		X_d/X_s
	0.6-1.0	1.0-1.8	0.6-1.0	1.0-1.8	Ratio
Tracking	1.7%	1.7%	1.7%	1.7%	
High-energy photon	2.5%	2.5%	2.5%	2.5%	
π^0/η reconstruction	1.7%	1.7%	1.7%	1.7%	
π^0/η veto	1.0%	1.0%	1.0%	1.0%	
K/π identification	2.0%	2.0%	2.0%	2.0%	2.0%
Neural network	5.0%	5.0%	5.0%	5.0%	
$B\bar{B}$ pair counting	1.1%	1.1%	1.1%	1.1%	
Fit PDFs	2.4%	3.6%	7.0%	8.3%	8.7%
Backgrounds	0.3%	0.4%	2.4%	6.1%	5.4%
Fit bias	0.4%	1.7%	0.4%	3.3%	3.0%
Fragmentation	3.6%		7.7%	8.5%	
Partial \mathcal{B}	7.0%	11.4%	10.0%	14.8%	13.8%
Missing ≥ 5 body		5.6%		25.8%	21.0%
Other missing states		17.0%		23.8%	7.1%
Spectrum Model		1.8%		1.6%	
Total \mathcal{B}	7.0%	21.2%	10.0%	38.1%	26.1%

to background ratios in the two samples. We vary the signal PDF parameters within the range allowed by the fit to the $B \rightarrow K^*\gamma$ data. The normalization of the signal cross-feed is varied by $\pm 30\%$, and the contribution of $B \rightarrow X\pi^0/\eta$ by $\pm 100\%$, in accordance with MC studies. The remaining peaking B backgrounds, including the $B \rightarrow X_s\gamma$ contribution in the $B \rightarrow X_d\gamma$ sample, are varied by $\pm 20\%$. We use simulated signal and background event samples to assign a systematic uncertainty due to the potential for bias in the fit method.

There is an additional systematic error on the efficiency due to the uncertainties in the measured fragmentation of the X_s hadronic system into the seven $B \rightarrow X_s\gamma$ final states. The equivalent error for $B \rightarrow X_d\gamma$ is obtained from the difference between our fragmentation model applied to $B \rightarrow X_d\gamma$ and the fragmentation observed in $B \rightarrow X_s\gamma$ data. We assume that these errors are independent and so do not cancel in the ratio of branching fractions.

Table IV also shows the systematic errors associated with correcting the partial branching fractions for the missing final states. There is no information from the data on the missing fraction of high multiplicity final states with ≥ 5 stable hadrons, or on the missing fraction of other final states with $\geq 1 \pi^0$ or η mesons. We vary these fractions by $\pm 50\%$ of their values from the default phase space fragmentation. We motivate our choice of a $\pm 50\%$ variation using signal models, for which we mix a combination of resonances as 50% fractions of $B \rightarrow X_s\gamma$ and $B \rightarrow X_d\gamma$ in the mass range $1.0 - 1.8 \text{ GeV}/c^2$. These give missing fractions close to the lower limits from the $\pm 50\%$ variations. The missing fraction errors partially cancel in the ratio when the $\pm 50\%$ variations are made in the same direction for $b \rightarrow d\gamma$ and $b \rightarrow s\gamma$.

We take the spectral shape of the high-energy photon from [12] with the kinetic parameters $(m_b, \mu_\pi^2) = (4.65 \text{ GeV}/c^2, -0.52 \text{ GeV}^2)$ extracted from fits to $b \rightarrow s\gamma$ and $b \rightarrow c\ell\nu$ data [13]. We vary these shape parameters in a correlated way between $(m_b, \mu_\pi^2) = (4.60 \text{ GeV}/c^2, -0.60 \text{ GeV}^2)$ and $(m_b, \mu_\pi^2) = (4.70 \text{ GeV}/c^2, -0.45 \text{ GeV}^2)$. There are systematic errors on the branching fractions from these variations, but they are small and cancel in the ratio. The fraction of the spectrum in the mass range $0.6-1.8 \text{ GeV}/c^2$ is $(51 \pm 4)\%$ for $b \rightarrow d\gamma$ and $(50 \pm 4)\%$ for $b \rightarrow s\gamma$. We do not extrapolate the ratio of branching fractions to $M_X > 1.8 \text{ GeV}/c^2$, so these errors, which mostly cancel in the ratio, are not included in Table IV. If we make this correction, we obtain $\mathcal{B}(b \rightarrow d\gamma) = (1.4 \pm 0.5 \pm 0.4 \pm 0.1) \times 10^{-5}$ and $\mathcal{B}(b \rightarrow s\gamma) = (4.3 \pm 0.3 \pm 0.7 \pm 0.2) \times 10^{-4}$, where the first error is statistical, the second systematic and the third accounts for the uncertainty in extrapolating to the full mass range. The result for $B \rightarrow X_s\gamma$ is consistent with the measured inclusive $b \rightarrow s\gamma$ branching fraction of $(3.55 \pm 0.24) \times 10^{-4}$ [11].

We convert the ratio of branching fractions from the full mass range $0.6-1.8 \text{ GeV}/c^2$, $\Gamma(b \rightarrow d\gamma)/\Gamma(b \rightarrow s\gamma) =$

$0.033 \pm 0.013 \pm 0.009$, into a value for $|V_{td}/V_{ts}|$ using Table 1 and Equation (26) of [3]. The result is $|V_{td}/V_{ts}| = 0.177 \pm 0.043 \pm 0.001$, where the first error is experimental, including systematic errors, and the second error is theoretical. The theoretical error includes uncertainties on the CKM parameters $\bar{\rho}$ and $\bar{\eta}$, and on $1/m_c^2$ and $1/m_b^2$ corrections, but does not include an uncertainty for the restriction of the measurement of the ratio to hadronic masses below $1.8 \text{ GeV}/c^2$.

As a check, we use the low mass region to determine $|V_{td}/V_{ts}|$ using predictions for exclusive $B \rightarrow (\rho, \omega)\gamma$ and $B \rightarrow K^*\gamma$ from [2]. We find $|V_{td}/V_{ts}| = 0.214 \pm 0.046 \pm 0.028$ where the first error is experimental and the second is theoretical. This is in good agreement with previously published results [1].

In summary we have made the first measurement of $B \rightarrow X_d\gamma$ decays in the hadronic mass range up to

$1.8 \text{ GeV}/c^2$, and have extracted $|V_{td}/V_{ts}|$ from an inclusive model with small theoretical uncertainties. These results are consistent with the measurements of $|V_{td}/V_{ts}|$ from the exclusive decays $B \rightarrow (\rho, \omega)\gamma$ [1], and with B_s/B_d oscillations [5].

We are grateful for the excellent luminosity and machine conditions provided by our PEP-II colleagues, and for the substantial dedicated effort from the computing organizations that support *BABAR*. The collaborating institutions wish to thank SLAC for its support and kind hospitality. This work is supported by DOE and NSF (USA), NSERC (Canada), CEA and CNRS-IN2P3 (France), BMBF and DFG (Germany), INFN (Italy), FOM (The Netherlands), NFR (Norway), MES (Russia), MEC (Spain), and STFC (United Kingdom). Individuals have received support from the Marie Curie EIF (European Union) and the A. P. Sloan Foundation.

-
- [1] B. Aubert *et al.* [BABAR Collaboration], Phys. Rev. Lett. **98**, 151802 (2007); D. Mohapatra *et al.* [Belle Collaboration], Phys. Rev. Lett. **96**, 221601 (2006).
 - [2] P. Ball, G. Jones and R. Zwicky, Phys. Rev. D **75**, 054004 (2007).
 - [3] A. Ali, H. Asatrian and C. Greub, Phys. Lett. B **429**, 87 (1998).
 - [4] S. Bertolini, F. Borzumati and A. Masiero, Nucl. Phys. B **294**, 321 (1987); H. Baer and M. Brhlik, Phys. Rev. D **55**, 3201 (1997); J. Hewett and J. Wells, Phys. Rev. D **55**, 5549 (1997); M. Carena *et al.*, Phys. Lett. B **499**, 141 (2001).
 - [5] W.-M. Yao *et al.*, J. Phys. G **33**, 1 (2006).
 - [6] B. Aubert *et al.* [BABAR Collaboration], Nucl. Instrum. Methods A **479**, 1 (2002).
 - [7] G. C. Fox and S. Wolfram, Nucl. Phys. B **149**, 413 (1979).
 - [8] B. Aubert *et al.* [BABAR Collaboration], Phys. Rev. Lett. **89**, 201802 (2002).
 - [9] H. Albrecht *et al.* [ARGUS Collaboration], Phys. Lett. B **185**, 218 (1987).
 - [10] T. Sjostrand, hep-ph/9508391; T. Sjostrand, Comput. Phys. Commun. **82**, 74 (1994).
 - [11] E. Barberio *et al.* [Heavy Flavor Averaging Group], arXiv:0704.3575 (hep-ex) (2007).
 - [12] A. L. Kagan and M. Neubert, Phys. Rev. D **58**, 094012 (1998).
 - [13] O. Buchmüller and H. Flächer, Phys. Rev. D **73**, 073008 (2006).